TEASING JETS IN p-p COLLISIONS AT ISR ENERGIES

F.L. Navarria*)
Istituto di Fisica dell'Università, Bologna, Italy
Istituto Nazionale di Fisica Nucleare, Sezione di Bologna, Italy

[CERN Experiment R412 **)]

Abstract: Recent evidence for jet-like structure in large p_T events observed in the central region at the CERN Intersecting Storage Rings (ISR) is presented.

Résumé : On présente des résultats, récemment obtenus aux ISR du CERN, en faveur d'une structure en "jet" des événements à grand p_T observés dans la région centrale.

*) Visitor at CERN, Geneva, Switzerland.

**) The other members of the collaboration are: P. Darriulat, P. Dittmann, K. Eggert, M. Holder, K.T. McDonald, T. Modis, A. Seiden, J. Strauss, G. Vesztergombi and E.G.H. Williams.

1. INTRODUCTION

Since the amazing discovery that the large p_T hadron-hadron inclusive cross-sections do not simply extrapolate the low p_T behaviour[1], much experimental and theoretical effort has been devoted to the understanding of this phenomenon with the aim of revealing elementary processes between hadron constituents at small distances[2,3]. At present the most appealing possibility is that large p_T events are due to hard collisions between point-like hadron constituents[4], qualitatively along the same line of thought of quark-parton models for deep-inelastic lepton-hadron processes. Although the theoretical difficulties of such a naive picture are many[3], the prediction of hard-scattering constituent models for p-p collisions is in general the presence of a coplanar, non-collinear, two-jet structure at large p_T which exhausts the transverse momentum balance. This jet structure would be of course washed out into a fan in experiments where many events are averaged over.

Studies of correlations in events with the requirement of a large p_T trigger particle [π^0's have been rather popular so far[2]] have provided the first hints towards a jet-like structure of the collisions by showing a rise in particle density compared to low p_T production over a wide angular range. The picture of the large p_T event emerging from the study of angular correlations can be summarized by three components[2]:

i) an underlying normal event, at all rapidities, with an $\exp(-6p_T)$ distribution, azimuthally symmetric, which corresponds to the low p_T behaviour at a centre-of-mass energy $\sqrt{s}_{eff} \sim \sqrt{s} - 2p_T^{trigger}$;

ii) jets on the same side of the trigger particle, confined in the angular range $\Delta\phi \sim 100°$, $\Delta y \sim 2$ units, and centred around the trigger particle;

iii) fans on the opposite side with $\Delta\phi \sim 180°$, $\Delta y \sim 4$ units, centred at $y = 0$.

Such an event structure is apparent in Fig. 1 which shows the angular correlations observed by the Aachen-CERN-Heidelberg-München Collaboration with $\theta_{trigger} = 90°$ and 53° in the c.m.s.[5]. However, this type of experiment has suffered in the past because of the lack of momentum measurement[5,6] or the limited solid angle[7], and therefore the most important question (i.e. How does the fan behave event-by-event? Does it look similar to the same side jet?) could not be answered.

The experiment[8] described here overcomes the above-mentioned difficulties by making use of a large solid angle detector with magnetic analysis, the CERN ISR Split-Field Magnet (SFM) facility[9].

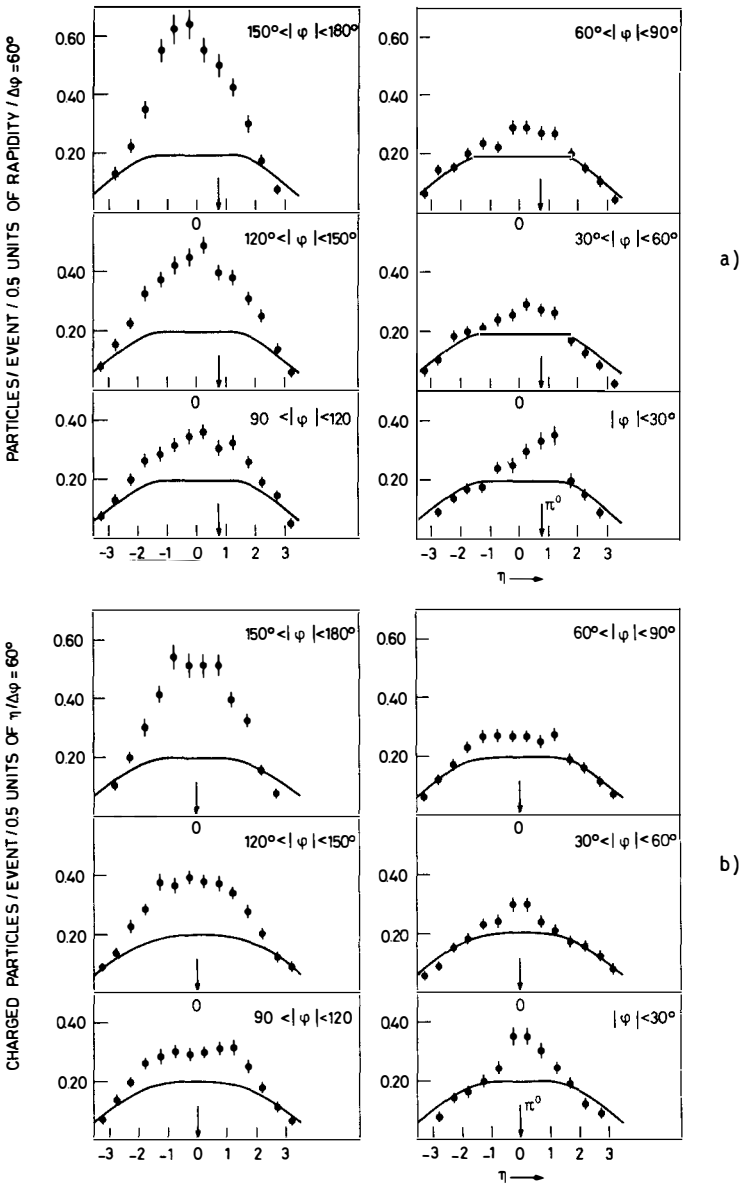

Fig. 1 Charged particle densities from ACHM data (Ref. 5) with $p_T^{\pi^0} > 2$ GeV/c; $\eta = -\ln \mathrm{tg}(\theta/2)$ is the psuedorapidity. The solid lines show charged particle densities in minimum bias (∿ inclusive) triggers: a) $\theta_{\pi^0} = 53°$, b) $\theta_{\pi^0} = 90°$.

2. SOME EXPERIMENTAL DETAILS

Figure 2 shows the top view of the apparatus used by the CERN R412 group. Since the experimental set-up and the methods are discussed in detail elsewhere[8], only the key features will be recalled here.

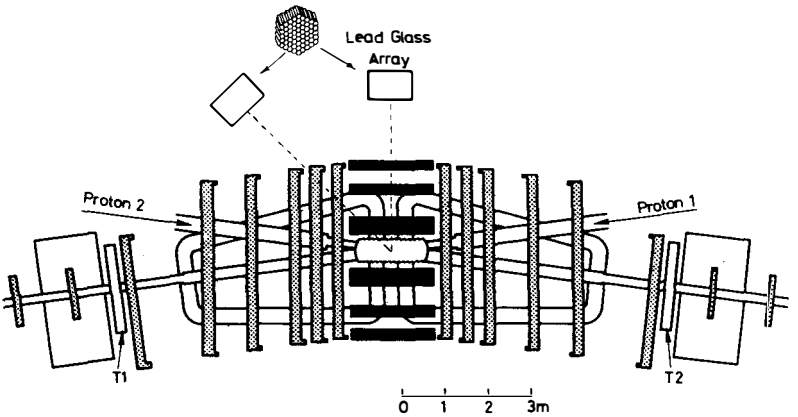

Fig. 2 Layout of the set-up used in the CERN R412 experiment. The forward (dotted) and the central (black) chambers of the SFM detector are shown. T1 and T2 are plastic scintillators used to detect small-angle secondaries. The two positions, $\theta = 90°$ and $\theta = 45°$, of the lead-glass array used to select the high $p_T^{\pi^0}$ trigger are indicated.

The large p_T trigger is provided by 1 m² lead-glass detector[10] positioned to accept π^0's emitted either at 90° or at 45° in the p-p centre-of-mass system. The π^0 is identified by requiring the $(\gamma\gamma)$ invariant mass to be compatible to m_{π^0} within the experimental resolution in the interval $2.0 < p_T^{\pi^0} < 4.1$ GeV/c. The average value of the transverse momentum is $\langle p_T^{\pi^0} \rangle = 2.45$ GeV/c.

Charged secondaries are momentum-analysed in the SFM multiwire proportional chamber detector[9]; no chambers were available below and above the intersect at the time of the experiment. The regions of good acceptance are:

$$\pi^0 \text{ hemisphere } (p_T > 400 \text{ MeV/c}) \quad \begin{cases} |y| \leq 2.0^{*)} \\ |\phi| \leq 27° \end{cases}$$

*) The rapidity $y = \frac{1}{2}\ln[(E + p_L)/(E - p_L)]$ is calculated assuming all particles to be pions.

$$\text{opposite hemisphere } (p_T > 200 \text{ MeV/c}) \begin{cases} |y| \leq 2.5 \\ |180° - \phi| \leq 35° \end{cases}.$$

Over this region, inefficiencies ($\sim$ 20%) due to interactions and decays, chambers' support lines and cuts in track-finding, have been corrected weighting the tracks by the inverse of their detection probability.

Data have been taken at $\sqrt{s}$ = 53 GeV and 45 GeV in the 90° position and at $\sqrt{s}$ = 45 GeV in the 45° position. Here, mainly the data at $\sqrt{s}$ = 53 GeV, $\theta_{\pi^0} = 90°$ [8] will be discussed, and to a lesser extent those at $\sqrt{s}$ = 45 GeV, $\theta_{\pi^0} = 45°$ [11].

Data have also been taken with a minimum bias trigger, using only the wire chamber information and the associated scintillators (no lead-glass in the trigger), to be used as reference in the comparison with large p_T events.

The inclusive behaviour is to be contrasted with the increase of particle multiplicity at all transverse momenta which is observed in large p_T events[8]. The excess over the minimum bias p_T distribution grows with p_T, both on the trigger side and in the opposite hemisphere, and is at least a factor five at p_T = 1.2 GeV/c, which will be the cut used here to define the fast particles participating in the high p_T process. Similar results, namely that also slow particles share the transverse momentum balance and that the excess increases dramatically with p_T, have been obtained previously by the CERN-Columbia-Rockefeller-Saclay Collaboration[7].

3. THREE HINTS FOR JETS

3.1 Jets along the direction of the large p_T trigger

The rapidity distributions of charged particles in the π^0 hemisphere and the corresponding ($\pi^0\pi^\pm$) mass distributions from the 90° data are shown in Fig. 3 for various p_x*) intervals between 0.4 and 1.7 GeV/c. Similar distributions from the 45° data are shown in Fig. 4. The relevant feature of the rapidity distributions is an excess of particle density, compared to minimum bias events, centred around the trigger direction, in agreement with previous observations[5,6]. This excess grows and shrinks with p_x, its integral being 0.13 ± 0.02 particles per event in the 90° data for $0.4 \leq p_x \leq 1.7$ GeV/c and $|\phi| \leq 27°$.

The angular shrinking of the correlated piece with increasing transverse momentum implies an associated mass distribution limited at low $\pi\pi$ masses:

*) p_x is the momentum component along the π^0 transverse momentum.

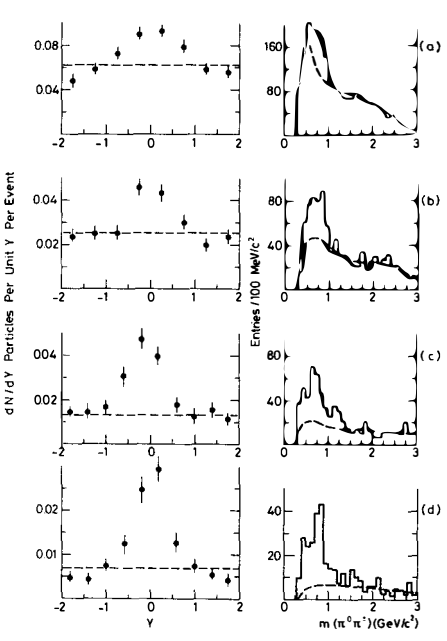

Fig. 3 90° data. Rapidity distributions and ($\pi^0\pi^\pm$) mass distributions for particles in the π^0 hemisphere: a) $0.4 \leq p_x < 0.6$, b) $0.6 \leq p_x < 0.8$, c) $0.8 \leq p_x < 1.1$, d) $1.1 \leq p_x < 1.7$ GeV/c. The dashed curves show the minimum bias rapidity distributions and the mass distributions expected for uncorrelated particles.

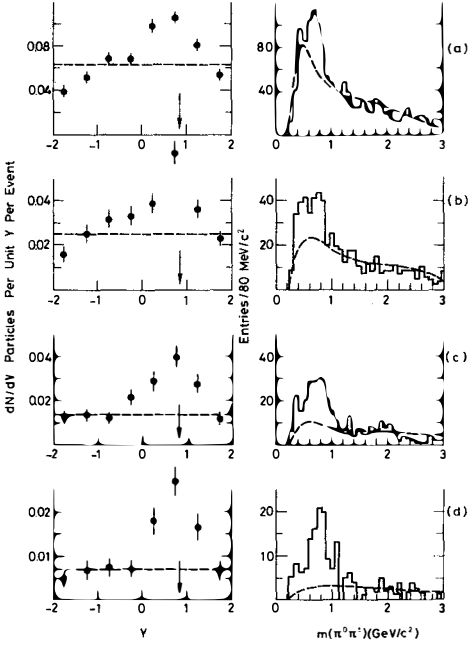

Fig. 4 Same as Fig. 3 for the 45° data.

this is clearly observed in Figs. 3 and 4 as a bump sitting over the background calculated from uncorrelated minimum bias distributions. The whole bump cannot be attributed to charged ρ meson productions since the mass resolution is about ±50 MeV: at large p_x, however, there is a clean signal at the ρ mass, consistent with the instrumental resolution and with the natural ρ decay width (see Fig. 5). By assuming that the ρ differential cross-section is a multiple of the π^0 cross-section, one obtains at 90° a cross-section ratio $\frac{1}{2}(\rho^+ + \rho^-)/\pi^0 = 0.9 \pm 0.2$ between ρ and direct π^0 production at an average transverse momentum $\langle p_T^\rho \rangle = \langle p_T^{\pi^0} \rangle = 3.5$ GeV/c.

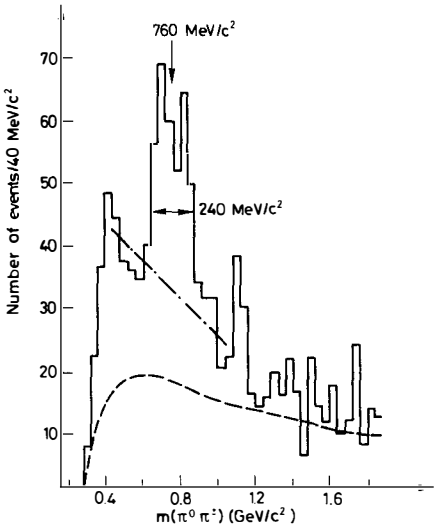

Fig. 5 $(\pi^0\pi^\pm)$ mass distribution for particles in the π^0 hemisphere with $0.7 < p_x^\pm < 1.7$ GeV/c (90° data). The dashed curve is the mass distribution expected for uncorrelated particles and the dashed-dotted line is the background assumed to estimate the ρ signal.

Since the ρ mesons do not exhaust the two-particle correlation and no evidence is found for large ω production ($\omega \to \pi^+\pi^-\pi^0/\pi^0 < 1$ at 95% confidence level at $\langle p_T^\omega \rangle = 3.5$ GeV/c), the natural question to ask is whether a three-particle correlation shows up for high p_x particles. By selecting a fast particle ($p_x > 1$ GeV/c) with rapidity around the π^0 rapidity and plotting the rapidity of all the other particles, a strong three-particle correlation is observed (see Fig. 6).

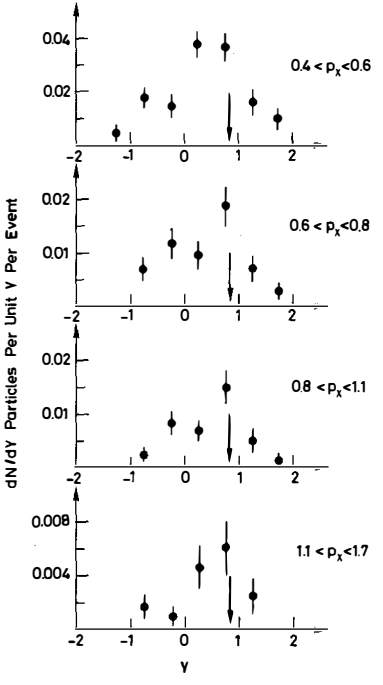

Fig. 6 Rapidity distribution of charged particles in the π^0 hemisphere from the 45° data. Secondaries from events in which a fast particle (p_x > 1 GeV/c, y > 0) occurs have been plotted; the fast particle is excluded from the plot.

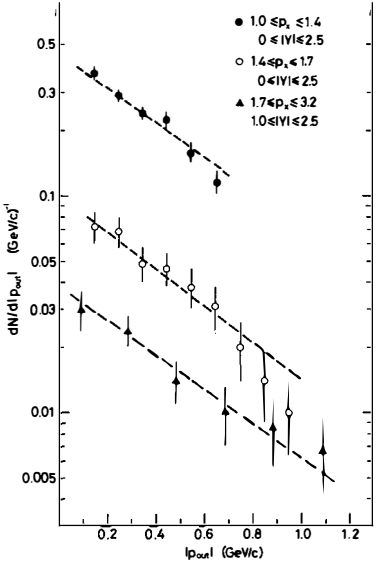

Fig. 7 Distributions of $|p_{out}|$ for different p_x intervals of the charged particles (90° data). The dashed lines show the result of a common fit: $dN/d|p_{out}| \propto \exp(-2|p_{out}|)$.

3.2 Coplanarity and transverse momentum sharing in the opposite hemisphere

The single-particle rapidity distribution in the hemisphere opposite the trigger has been studied[8] as a function of charge, p_x and $p_T^{\pi^0}$, and it has been found to follow the well-known fan-like behaviour[5,6] with an overall particle density increase at all p_x roughly linear with $p_T^{\pi^0}$. The distributions are independent of charge, the +/- charge ratio being about 1.2, apart from the large p_x, large y region where the +/- ratio increases to about 2, qualitatively in a similar way to what is observed in inclusive distributions[12].

The important point to emphasize in order to test the jet structure in single-particle distributions is the coplanarity with the scatter plane defined by the trigger and the incoming protons. The distributions in the momentum component orthogonal to the scatter plane, p_{out}, are shown in Fig. 7 for various p_x intervals ranging from 1.0 to 3.2 GeV/c. The result is that the p_{out} distribution turns out to be independent of p_x, whilst from minimum bias events we expect

$$\langle p_{out} \rangle \simeq 0.6\sqrt{p_x} \quad (p_{out},\ p_x \text{ in GeV/c}) \ .$$

An empirical fit of the form

$$dN/d|p_{out}| = A \exp(-B\ |p_{out}|)$$

gives an excellent χ^2 and an average $\langle p_{out} \rangle = 1/B = (0.50 \pm 0.05)$ GeV/c (see Table 1). By studying the p_{out} distribution in various rapidity intervals and separately for + and - charges, $\langle p_{out} \rangle$ is found to be the same within errors and the p_{out} distribution is shown to factorize.

Table 1

Fits to the p_{out} distributions

p_x range (GeV/c)	$\langle \lvert p_x \rvert \rangle$	$B = 1/\langle \lvert p_{out} \rvert \rangle$ $(\text{GeV/c})^{-1}$	χ^2/DF
$1.0 \leq p_x < 1.43$	1.17	2.1 ± 0.2	0.9
$1.43 \leq p_x < 1.72$	1.54	2.3 ± 0.3	0.4
$1.72 \leq p_x \leq 3.2$	2.13	1.7 ± 0.4	0.3

Since the coplanarity between the trigger plane and the particles emitted with azimuth opposite to the trigger is indicated by the limited p_{out}, it is interesting to understand how the transverse momentum is balanced in the large p_T process. To do this we consider the distribution in

$x_E = |p_x/p_T^{\pi^0}|$ for fast particles ($p_x > 1.2$ GeV/c) presumably linked to the high p_T process with little background. Figure 8a shows the x_E distributions from the $\theta_{\pi^0} = 90°$ and $\theta_{\pi^0} = 45°$ data, after correcting for the unseen p_{out} region. These distributions are equal within errors, as is expected from hard-scattering models if there is not a strong θ dependence in the c.m.s. of the colliding constituents. The x_E distribution is steeply falling and has an integral of about 0.25 for $x_E \geq 0.4$, i.e. on the average 25% of the events have a charged particle which balances more than 40% of the trigger π^0 transverse momentum by itself.

The assumption that the π^0 carries all the relevant p_T in its hemisphere ($p_T^{\pi^0} = p_T^{jet}$, say) may be questioned since particles correlated with the π^0 are clearly observed (see Section 3.1), and this correlation increases with the x_E in the opposite hemisphere (see Table 2). To test this assumption we show in Fig. 8b the distribution in $x'_E = |p_x/(p_T^{\pi^0} + p'_x)|$, where $p'_x \neq 0$ for the fraction of events with a particle close to the π^0 ($|y'| < 1$ and $p'_x > 0.4$ GeV/c): the conclusion is that the x'_E distribution does not differ seriously from the x_E distribution.

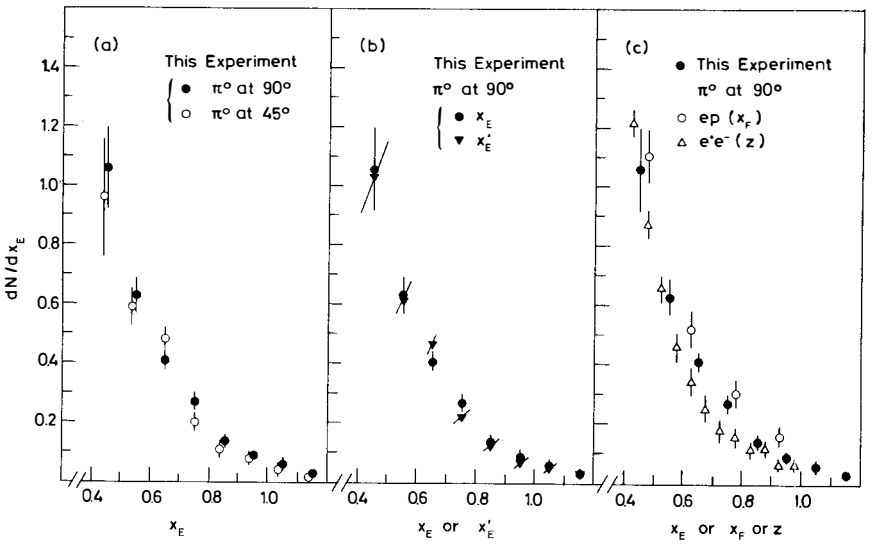

Fig. 8 a) The x_E distributions obtained from the 90° and from the 45° data. b) Comparison between the x_E and the x'_E distributions (90° data). c) The x_E distribution (90° data) is compared with the Feynmann x_F distribution observed in deep-inelastic e-p scattering (Ref. 13) and with $\frac{1}{2}dN/dz$ ($z = p/p_{max}$) observed in e^+e^- annihilations at $E_{cm} = 4.8$ GeV/c (Ref. 14).

Table 2

Percentage of events with a fast particle correlated to the π^0 ($|y| < 0.5$, $p_X > 1$ GeV/c) versus x_E, of the fastest particle in the opposite hemisphere (90° data).

x_E range	%
All events	4.5 ± 0.5
0.4-0.6 ($p_X > 1.2$ GeV/c)	7.8 ± 1.6
Above 0.85	13.6 ± 3.9

A comparison between the x_E distribution and the fractional hadron momentum distribution observed in deep inelastic e-p scattering[13] and in e^+e^- annihilations[14] is shown in Fig. 8c. All these distributions are again similar in shape and magnitude, a result which is expected in quark-parton models where the hadrons in the final state are interpreted to be the fragments of a large transverse momentum quark.

3.3 Rapidity correlations in the hemisphere opposite the large p_T trigger (towards unfolding the fan)

Further evidence for an event-by-event jet-like structure comes from the study of rapidity correlations in the hemisphere opposite the trigger. This is done by selecting events with a fast particle ($p_x > 1.2$ GeV/c) in different rapidity intervals and plotting the rapidity distribution of the other secondaries irrespective of their momenta, as shown in Fig. 9. The density of particles accompanying a large x_E particle is seen to shift in rapidity towards its direction, in such a way that a fraction of the particles is closely correlated to the largest x_E particle and another fraction is more or less uniformly distributed over the available rapidity range. This compares well with what is observed on the trigger side in the ACHM data[5], where no momentum analysis was available (see Fig. 1). Figure 10 shows the average additional charged particle densities when selecting a) the fastest particle ($p_x > 1.2$ GeV/c at least), b) a random slow particle ($p_x < 0.6$ GeV/c). Both distributions can be decomposed into an excess centred at $\Delta y = 0$ and a background proportional to the uncorrelated particle density. The correlated piece is narrower when selecting fast particles, ±0.6 units of rapidity versus ±0.8, and contains more particles per event, 0.33 ± 0.07 versus 0.18 ± 0.03.

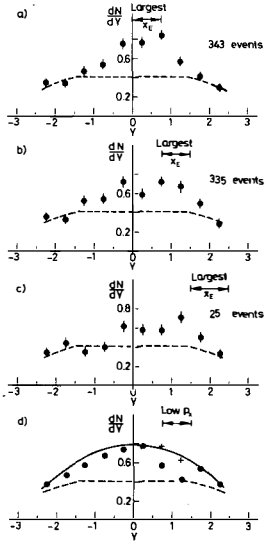

Fig. 9 Associated charged particle rapidity distributions in the hemisphere opposite the π^0 (90° data). a), b), and c) selecting events with the largest x_E particle (not plotted) in different rapidity intervals. d) selecting events with a low p_x particle (p_x < 0.6 GeV/c, not plotted). The dashed lines show the minimum bias distribution and the solid line shows the distribution observed in an average high $p_T^{\pi^0}$ event.

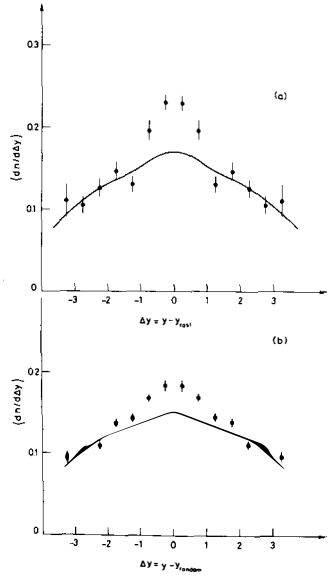

Fig. 10 a) Average particle density of charged secondaries in events where a fast particle (p_x > 1.2 GeV/c) occurs. The particle density, which is a function of y and y_{fast}, has been averaged over $y + y_{fast}$. The solid line has the shape of the uncorrelated particle density and is normalized to the points at large Δy. b) Same distributions as in (a), but selecting the reference particle at random among secondaries with p_x < 0.6 GeV/c.

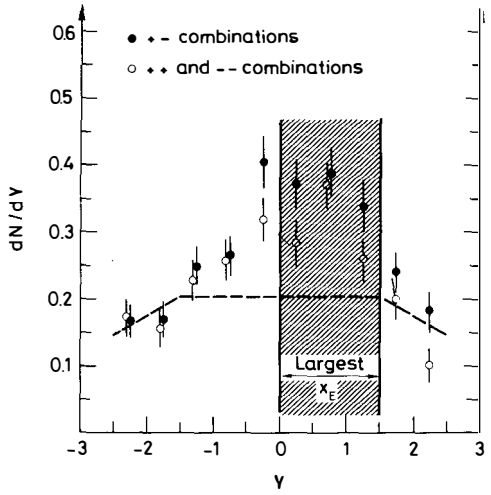

Fig. 11 Same distributions as in Fig. 9, but selecting secondaries with charge equal or opposite to the largest x_E particle (90° data).

The fact that, with a large p_T trigger, the request of a fast particle in the opposite hemisphere enhances and shrinks the short-range rapidity correlation as compared to the selection of low p_T secondaries, is new and points to some intrinsic similarity between the side of the trigger and the opposite side.

Since the only quantum number which can be studied in the present experiment is charge, we display in Fig. 11 the charge content of the excess of correlated particles. It is found that the excess consists of 1/3 of the secondaries with charge equal to the large x_E particle, and of 2/3 of the secondaries with charge opposite to the large x_E particle. Similar short-range charge correlations have been studied in inclusive events[15] leading to similar results.

The final question is to see whether the uncorrelated background can be further reduced by asking the secondaries to have also a large transverse momentum. Figure 12 shows the rapidity distributions of particles with $p_x > 0.8$ GeV/c in events where a large x_E particle ($p_x > 1.2$ GeV/c) is present. A background calculated under the assumption that the largest x_E product and the high p_x secondary are uncorrelated and follow the $p_T^{\pi^0}$ spectrum and the minimum bias distribution, respectively, reproduces well the low background observed and leaves an excess of 0.15 ± 0.06 particles per event over a narrow rapidity range.

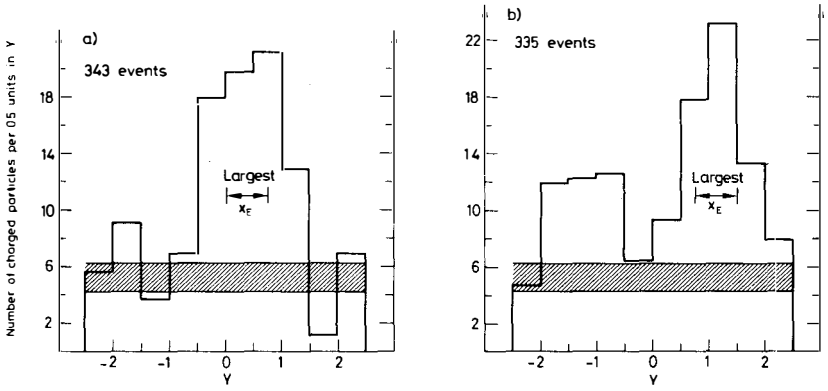

Fig. 12 Rapidity distribution of high p_x charged secondaries ($p_x > 0.8$ GeV/c) from events in which the largest x_E particle (not plotted) is within the intervals: a) $0 \leq y < 0.75$, b) $0.75 \leq y \leq 1.5$. The cross-hatched area is the distribution described in the text.

4. CONCLUSIONS

All the correlation features presented above for particles accompanying a high p_T particle in the hemisphere opposite the trigger π^0 are qualitatively very similar to the features seen for particles accompanying the π^0 in its hemisphere. This evidence for narrow rapidity clustering on both sides, in addition to the coplanarity structure of the large p_T event and to the transverse momentum distribution in the opposite hemisphere, conspires towards a coplanar two-jet picture of large p_T p-p collisions in analogy with what is found in deep inelastic lepton-proton and e^+e^- collisions. This coplanar two-jet structure is always superimposed on the underlying behaviour of the normal low p_T "background" event.

Needless to say, much more experimental work is required in several directions before firmly establishing the picture outlined above. Let us list a few points: i) transverse momentum larger than in the present experiment have to be studied; ii) quantum number correlations have to be investigated (e.g. identifying baryons and strange particles); and iii) it might be useful to trigger the large p_T event with a large solid-angle calorimeter in order not to single out a possibly special jet.

* * *

REFERENCES

1) B. Alper et al., Phys. Letters 44B, 521 (1973).
M. Banner et al., Phys. Letters 44B, 537 (1973).
F.W. Büsser et al., Phys. Letters 46B, 471 (1973).
J.W. Cronin et al., Phys. Rev. Letters 31, 1426 (1973).
D.C. Carey et al., Phys. Rev. Letters 32, 24 (1974).

2) For a review of the experimental data, see P. Darriulat, Hadronic collisions with a large transverse momentum product, Rapporteur talk at the EPS Internat. Conf. on High-Energy Physics, Palermo, 23-28 June 1975.

3) S.D. Ellis, Theoretical models for large transverse momentum phenomena, Proc. 17th Internat. Conf. on High-Energy Physics, London, 1974 (Science Research Council, RHEL, Didcot, UK, 1974), p. V-23.
P.V. Landshoff, Plenary Report on large transverse momentum reactions, ibid., p. V-57.
D. Sivers, S.J. Brodsky and R. Blankenbecler, Phys. Reports 23C, 1 (1976).

4) S.M. Berman, J.D. Bjorken and J.B. Kogut, Phys. Rev. D 4, 3388 (1971).

5) Aachen-CERN-Heidelberg-München Collaboration, K. Eggert et al., Nuclear Phys. B98, 73 (1975).

6) Pisa-Stony Brook Collaboration, G. Finocchiaro et al., Phys. Letters 50B, 396 (1974).

7) CERN-Columbia-Rockefeller Collaboration, F.W. Büsser et al., Phys. Letters 51B, 306 and 311 (1974).
CERN-Columbia-Rockefeller-Saclay Collaboration, F.W. Büsser et al., A study of inclusive spectra and two particle correlations at large transverse momentum, January 1976, to be published in Nuclear Phys. B.
Aachen-CERN-Heidelberg-München Collaboration, K. Eggert et al., Nuclear Phys. B98, 49 (1975).

8) P. Darriulat et al., Structure of final states with a high transverse momentum π^0 in proton-proton collisions, February 1976, to be published in Nuclear Phys. B.

9) R. Bouclier et al., Nuclear Instrum. Methods 115, 235 (1974).
R. Bouclier et al., Nuclear Instrum. Methods 125, 19 (1975).

10) M. Holder et al., Nuclear Instrum. Methods 108, 541 (1973).

11) A preliminary report on the 45° data has been given by J. Strauss, see ISR Discussion Meeting between Experimentalist and Theorists, Summary 17, November 1975, unpublished.

12) P. Capiluppi et al., Nuclear Phys. B79, 189 (1974).

13) J.T. Dakin et al., Phys. Rev. D 10, 1401 (1974).

14) B. Richter, Plenary Report on $e^+e^- \to$ hadrons, Proc. 17th Internat. Conf. on High-Energy Physics, London, 1974 (Science Research Council, RHEL, Didcot, UK, 1974), p. IV-37.
R. Hollebeek, LBL 3874 (May 1975), unpublished.

15) Notre Dame-Duke-Toronto-McGill Collaboration, N.N. Biswas et al., Phys. Rev. Letters 35, 1059 (1975).